The First Crystal Structure of a Thioacylenzyme Intermediate in the ALDH Family: New Coenzyme Conformation and Relevance to Catalysis†

Katia D'Ambrosio,‡,§ Arnaud Pailot,|| François Talfournier,|| Claude Didierjean,‡ Ettore Benedetti,§ André Aubry,‡ Guy Branlant,*,|| and Catherine Corbier*,‡

LCM3B, Groupe Biocristallographie, UMR 7036, CNRS-UHP, Faculté des Sciences, 54506 Vandoeuvre Cedex, France, Istituto di Biostrutture e Bioimmagini, CNR, Dipartimento delle Scienze Biologica, Università degli Studi di Napoli "Federico II", 80134 Napoli, Italia, and MAEM, UMR 7567, CNRS-UHP, Faculté des Sciences, 54506 Vandoeuvre Cedex, France

Received July 29, 2005; Revised Manuscript Received January 3, 2006

ABSTRACT: Crystal structures of several members of the nonphosphorylating CoA-independent aldehyde dehydrogenase (ALDH) family have shown that the peculiar binding mode of the cofactor to the Rossmann fold results in a conformational flexibility for the nicotinamide moiety of the cofactor. This has been hypothesized to constitute an essential feature of the catalytic mechanism because the conformation of the cofactor required for the acylation step is not appropriate for the deacylation step. In the present study, the structure of a reaction intermediate of the E268A-glyceraldehyde 3-phosphate dehydrogenase (GAPN) from *Streptococcus mutans*, obtained by soaking the crystals of the enzyme/NADP complex with the natural substrate, is reported. The substrate is bound covalently in the four monomers and presents the geometric characteristics expected for a thioacylenzyme intermediate. Control experiments assessed that reduction of the coenzyme has occurred within the crystal. The structure reveals that reduction of the cofactor upon acylation leads to an extensive motion of the nicotinamide moiety with a flip of the reduced pyridinium ring away from the active site without significant changes of the protein structure. This event positions the reduced nicotinamide moiety in a pocket that likely constitutes the exit door for NADPH. Arguments are provided that the structure reported here constitutes a reasonable picture of the first thioacylenzyme intermediate characterized thus far in the ALDH family and that the position of the reduced nicotinamide moiety observed in GAPN is the one suitable for the deacylation step within all of the nonphosphorylating CoA-independent ALDH family.

Two phylogenetically and structurally unrelated families of NAD(P)-dependent aldehyde dehydrogenases (ALDH)[1] catalyze the oxidation of aldehydes into activated or nonactivated acids. These enzymes are known to be involved in many biological functions such as cellular differentiation, central metabolism, or detoxification pathways. They share a similar chemical mechanism involving two major steps: first, an acylation step common to both families and, second, a deacylation step that differs by the nature of the acyl-acceptor. The acylation step includes the formation of a thiohemiacetal intermediate via a nucleophilic attack of the catalytic cysteine on the aldehydic function followed by an oxidoreduction process leading to the formation of a thioacylenzyme intermediate and NAD(P)H. In the phosphorylating ALDH family, inorganic phosphate acts as an acyl-acceptor, thus leading to the formation of phosphor-esters, whereas in the nonphosphorylating ALDH family, the thioacylenzyme intermediate undergoes a nucleophilic attack by either a water molecule or a coenzyme A (CoA) molecule, thus leading to either nonactivated or CoA-activated acids, respectively. Moreover, previous studies have highlighted major differences in the kinetic mechanism of ALDHs depending upon the nature of the deacylation step following the oxido-reduction process. In the phosphorylating and nonphosphorylating CoA-dependent ALDHs, kinetic data support a ping-pong mechanism in which the release of the reduced cofactor occurs prior to the deacylation step, i.e., phosphorolysis or transthioesterification (*1*−*3*). The picture is clearly different for the nonphosphorylating CoA-independent ALDHs, which exhibit an ordered sequential mechanism in which NAD(P)H dissociates last (*4*, *5*). The fact that the cofactor remains bound to the enzyme along the two-step catalytic mechanism imposes the reduced nicotinamide mononucleotide (NMNH) moiety to move away from the initial position of the nicotinamide mononucleotide

† This research was supported by the Centre National de la Recherche Scientifique, the French Ministère de la Recherche et de l'Enseignement Supérieur, the University Henri Poincaré Nancy I, the IFR 111 Bioingénierie, and local funds from the Région Lorraine.

* To whom correspondence should be addressed: MAEM, UMR 7567, CNRS-UHP, Faculté des Sciences, 54506 Vandoeuvre Cedex, France. Telephone: +33 3 83 68 43 04. Fax: +33 3 83 68 43 07. E-mail: guy.branlant@maem.uhp-nancy.fr (G.B.); LCM3B, Groupe Biocristallographie, UMR 7036, CNRS-UHP, Faculté des Sciences, 54506 Vandoeuvre Cedex, France. Telephone: +33 3 83 68 47 89. Fax: +33 3 83 40 64 92. E-mail: catherine.corbier@lcm3b.uhp-nancy.fr (C.C.).

‡ LCM3B.

§ Università degli Studi di Napoli "Federico II".

|| MAEM.

[1] Abbreviations: GAPN, nonphosphorylating glyceraldehyde-3-phosphate dehydrogenase; ALDH, aldehyde dehydrogenase; CoA, coenzyme A; NMN(H), nicotinamide mononucleotide oxidized form (reduced form); D-G3P, D-glyceraldehyde-3-phosphate; PEG, poly(ethylene glycol).

10.1021/bi0515117 CCC: $33.50 © 2006 American Chemical Society
Published on Web 02/07/2006

(NMN) moiety for permitting the deacylation to occur (see the next paragraph).

Mechanistic aspects were studied extensively, and several invariant residues were shown to be critical for the chemical mechanism of nonphosphorylating CoA-independent ALDHs (*6*−*9*). More recently, evidence was put forward for the chemical activation of the catalytic C302 upon cofactor binding to nonphosphorylating glyceraldehyde-3-phosphate dehydrogenase (GAPN) from *Streptococcus mutans* (*10*). Moreover, additional studies on GAPN have highlighted the essential roles of (i) an oxyanion hole composed of at least the side chain of the invariant N169 residue that allows an efficient hydride transfer without base catalyst assistance (*11*, *12*) and (ii) the E268 residue in the rate-limiting hydrolysis step through activation and orientation of the attacking water molecule (*4*). From these results, a scenario for the chemical catalysis of GAPN was proposed (*4*). Additionally, numerous crystal structures of CoA-independent ALDHs have already been solved in the presence of NAD(P). One of the most striking features of these structures is the conformational flexibility of the NMN moiety of the cofactor (e.g., see refs *13*−*15*). Specifically, two distinct conformations were described for class 1 and class 2 ALDHs. In one conformation, the NMN moiety occupies a position suitable for hydride transfer, while it blocks the way and prevents the catalytic E268 from playing its role in the deacylation step. In contrast, the second conformation in which the NMN moiety moves away from the active site would be suitable for deacylation (*16*, *17*). This observation suggested that movement of the NMNH is a prerequisite for the deacylation. In a recent study, the crystal structures of wild-type and C302S human mitochondrial ALDHs, in binary complexes with NAD^+ and NADH, have led the authors to assign a preferential conformation of the cofactor related to its redox state; i.e., NAD^+ would adopt a conformation suitable for hydride transfer, whereas NADH would prefer a contracted conformation suitable for the deacylation process (*18*). However, recent structural data on GAPN from *Thermoproteus tenax* in complex with its cosubstrate NAD^+ or its inhibitor NADPH showed that both cofactors adopt a hydride-transfer conformation (*19*). This result suggested that the redox state of the cofactor is not necessarily the key factor triggering this isomerization step.

In the present study, an approach is described that provides for the first time structural evidence for a conformational isomerization of the cofactor during the catalytic cycle of a nonphosphorylating CoA-independent ALDH. For this purpose, we took advantage of the well-characterized kinetic properties of the E268A−GAPN from *S. mutans*, which showed that substituting Ala for Glu did not significantly affect the acylation rate but drastically reduced the deacylation rate by 3 orders of magnitude (*4*). Diffusion of the substrate in the crystalline binary complex GAPN−$NADP^+$ allowed the accumulation and trapping of the thioacylenzyme intermediate within the crystal. The structure reveals an extensive motion of the NMNH moiety of the cofactor after the acylation step and clearly establishes that cofactor isomerization is a prerequisite for the two-step mechanism to occur in nonphosphorylating CoA-independent ALDHs. The data are discussed in relation to previous structural and kinetic studies on GAPN and from an evolutionary viewpoint.

Table 1: Data Collection and Refinement Statistics[a]

data collection	
space group	$P2_12_12$
a (Å)	142.5
b (Å)	154.9
c (Å)	112.5
Z	4
resolution (Å)	2.55
outermost resolution shell (Å)	2.61−2.55
temperature (K)	100
total reflections	452 200
unique reflections	79 121
completeness (%)	97.4 (87.9)
R sym (%)	7.4 (24.2)
mean $I/\sigma(I)$	16.9 (3.2)
refinement	
R factor (%)	19.8 (26.5)
R free (%)	24.8 (32.2)
rmsd from ideal geometry	
bond lengths (Å)	0.006
bond angles (deg)	1.33
average *B* factor (Å^2)	
all atoms	34.4
protein atoms (14 392)	34.0
water molecules (776)	34.7
NADPH (adenosine 2′ 5′ P moiety)	48.01
NADPH (NMNH moiety)	53.76
G3P	38.7

[a] Values in parentheses in column 2 refer to the outermost resolution shell.

EXPERIMENTAL PROCEDURES

The E268A−GAPN enzyme was produced and purified as already described (*11*). Its concentration was determined spectrophotometrically as the apo form by using a molar extinction coefficient of 2.04×10^5 M^{-1} cm^{-1}. D-Glyceraldehyde-3-phosphate (D-G3P; Sigma, St. Louis, MO) was prepared from the D-G3P diethylacetal according to the manufacturer, and its concentration was assessed enzymatically using the wild-type GAPN.

Crystallization, Data Collection, and Processing. Crystals of the E268A−GAPN with $NADP^+$ were obtained using the hanging drop vapor diffusion method at 293 K. A total of 1 μL of a 70 mg/mL protein solution in 50 mM imidazole buffer at pH 6.8 containing 16 mM of $NADP^+$ was mixed with 2 μL of reservoir solution composed of 0.8 M sodium formate, 7% (w/v) poly(ethylene glycol) (PEG) 8000, 10% (w/v) PEG 1000, and 0.1 M imidazole (pH 6.8). The crystals grew within a few days. The thioacylenzyme intermediate was obtained by soaking the crystals in a solution containing 0.5 mM D-G3P for 20 min. A 2.55 Å resolution data set was collected at 100 K on beam line BM30A at ESRF, Grenoble, France (FIP, *20*). The crystals belong to the space group $P2_12_12$, with unit cell dimensions $a = 142.5$ Å, $b = 154.9$ Å, and $c = 112.5$ Å. Diffracted data were processed using the HKL crystallographic data reduction package (*21*). Statistics of the data set are summarized in Table 1.

Phasing and Refinement. The structure of the thioacylenzyme intermediate was solved by molecular replacement using the wild-type holoenzyme structure as a starting model (PDB code 2euh) (*15*). Refinement and manual rebuilding were carried out with CNS (*22*) and TURBO−FRODO (*23*), respectively. Fourier maps calculated with $(3F_o - 2F_c)$ and $(F_o - F_c)$ coefficients showed prominent electron-density features in the active-site region. The four monomers of the asymmetric unit were refined without imposing noncrystal-

lographic symmetry restraints. After initial refinement, limited to the enzyme, a model for D-glyceraldehyde moiety acylating C302 was built and introduced into the atomic coordinates set for further refinement. After several cycles of positional and *B*-factor crystallographic refinement, the analysis of the electron-density maps suggested the presence of a double conformation for both the catalytic C302 and the cofactor molecule into each subunit, which were each best-refined with an occupancy factor of 0.5 (see the Results). The ordered water molecules were added automatically and checked individually. Each peak contoured at 3σ in the ($F_o - F_c$) maps was identified as a water molecule, provided that hydrogen bonds would be allowed between this site and the model. The final crystallographic *R*-factor and *R*-free values calculated for the 79 121 independent reflections (in the 20.00−2.55 Å resolution range) were 0.198 and 0.248, respectively. The stereochemical quality of the model was assessed by PROCHECK (*24*). The most favored and additionally allowed regions of the Ramachandran plot contained 99.6% of the nonglycine residues. The statistics for refinement and model geometry are summarized in Table 1. Coordinates and structure factors have been deposited in the Protein Data Bank at the Research Collaboratory for Structural Bioinformatics (accession code 2ESD). Figures 1A, 2, and 3 were drawn using BOBSCRIPT (*25*), and Figures 1B, 4, and 5 were drawn with MOLMOL (*26*).

Redox State of the Cofactor within the Crystals. Characterization of the redox state of the cofactor within the crystal was carried out by quantification of the NADPH/$NADP^+$ ratio by high-pressure liquid chromatography. Crystals were washed to remove any excess of D-G3P and $NADP^+$ and then dissolved in acetonitrile (20%), and finally, the GAPN protein was eliminated by centrifugation at 4000*g* for 10 min at 4 °C. The supernatant was injected onto a Source 15Q anionic column using an ÄKTA Explorer system (Amersham Pharmacia Biotech) previously equilibrated with H_2O. $NADP^+$ and NADPH were eluted at 160 and 270 mM, respectively, with a linear gradient of 0−1 M KCl in H_2O at 1 mL/min.

RESULTS

Strategy Used To Obtain the Thioacylenzyme Intermediate. Albeit crystals of the wild-type enzyme have previously been obtained in the presence of ammonium sulfate as a precipitating agent, these conditions were not suitable in the present study because ammonium sulfate might compete with the phosphate of G3P and also because the pH value (ca 5) was too low. Indeed, the active-site C302 (pK_a value 6.1) has to be under the thiolate form to allow an efficient acylation step. New crystallization conditions have therefore been set up, using the approach proposed by Brzozowski et al. (*27*). The pH of the crystallization medium has been chosen and fixed at a value of 6.8 higher than the pK_a value of C302 and in a range where the deacylation rate is slow enough (*4*) to allow the accumulation of the thioacylenzyme intermediate within the crystal. Orthorhombic crystals have been obtained using a mixture of PEG 8000 (7%) and 1000 (10%) in 100 mM imidazole buffer as a precipitant; they belong to space group $P2_12_12$ and contain one tetramer per asymmetric unit. These crystals are isomorphous to those of the wild-type holoenzyme obtained in a different crystallization condition (*15*) and diffract at the same moderate resolution (2.55 Å).

Overall Structure of the Ternary Complex and Comparison with the Wild-Type Holoform. As found for the wild-type holo form (*15*), the E268A−GAPN from *S. mutans* in the ternary complex exists as a tetramer with four identical subunits related by a noncrystallographic 222 symmetry. Each monomer can be divided into three domains: a cofactor binding domain, composed of a *core* that resembles the Rossmann fold (*28*) (residues 145−252) flanked by five α helices and four β strands (residues 2−118 and 450−464), a catalytic α/β domain (residues 253−449), and a small β-stranded protruding domain, which enables oligomerization (residues 119−144 and 465−475).

No significant structural differences are observed between the four monomers of the E268A−GAPN structure, as illustrated by the low global root-mean-square deviation (rmsd) value (0.15−0.26 Å) calculated for the superimposition of the 474 Cα atoms. The main differences are located in the N- and C-terminal regions and in regions involved in the interaction between symmetry-related molecules. In particular, higher displacements are found for residues N339−E351, corresponding to the loop connecting α_{11} helix to the β_Q strand (for nomenclature of the secondary structures, see ref *15*). This region is located at the protein surface and is involved in crystal packing in monomers A and C. Because the structures of both wild-type and E268A−GAPNs reveal a quasi-perfect 222 symmetry, the least-squares superimpositions involving the 474 Cα atoms of the subunit A of the wild-type holoenzyme (*15*) (PDB code 2euh) were realized with each subunit of the E268A−GAPN. The resulting rmsd values are less than 0.41 Å, showing that the overall structure of the E268A−GAPN is very close to that of the wild-type holoenzyme. Local differences, with values higher than 3 times the rmsd value, are only observed for solvent-exposed residues or regions involved in the crystal packing.

Active Site. In each monomer, the first calculated difference electron-density map already exhibited a strong positive density peak in line with the catalytic C302 sulfur atom, the shape of which was consistent with the presence of a substrate molecule. Nevertheless, it appeared clearly during the refinement steps that the catalytic C302 adopts a double conformation that can be observed in each of the four monomers. The first conformation is superimposable to that found in the wild-type enzyme/NADP binary complex (*15*), and in this conformation, C302 forms a covalent linkage with the substrate. The second one is that found in the apo form (*15*), and in this one, no substrate is present (Figure 1A). These two conformations were satisfactorily refined with an occupancy factor of 0.5. The substrate adopts the same position in all of the four monomers and is well-defined in the ($3F_o - 2F_c$) electron-density map (Figure 1A). The continuous electron density from the C302−SG atom to the C1 atom of the substrate highly suggests the presence of a covalent bond, and the flat density shape at C1 satisfies a sp^2 hybridization. Both observations are those expected for a thioacylenzyme intermediate. Furthermore, analysis of the redox state of the cofactor confirmed that acylation has indeed occurred within the crystals (see below). The oxygen atom of the carbonyl group at C1 is hydrogen-bonded to the C302 amide nitrogen (2.75 Å) and to the N169−ND_2 atom (2.75 Å), two groups formerly postulated to be involved in the formation of the oxyanion hole. The oxygen atom at C2

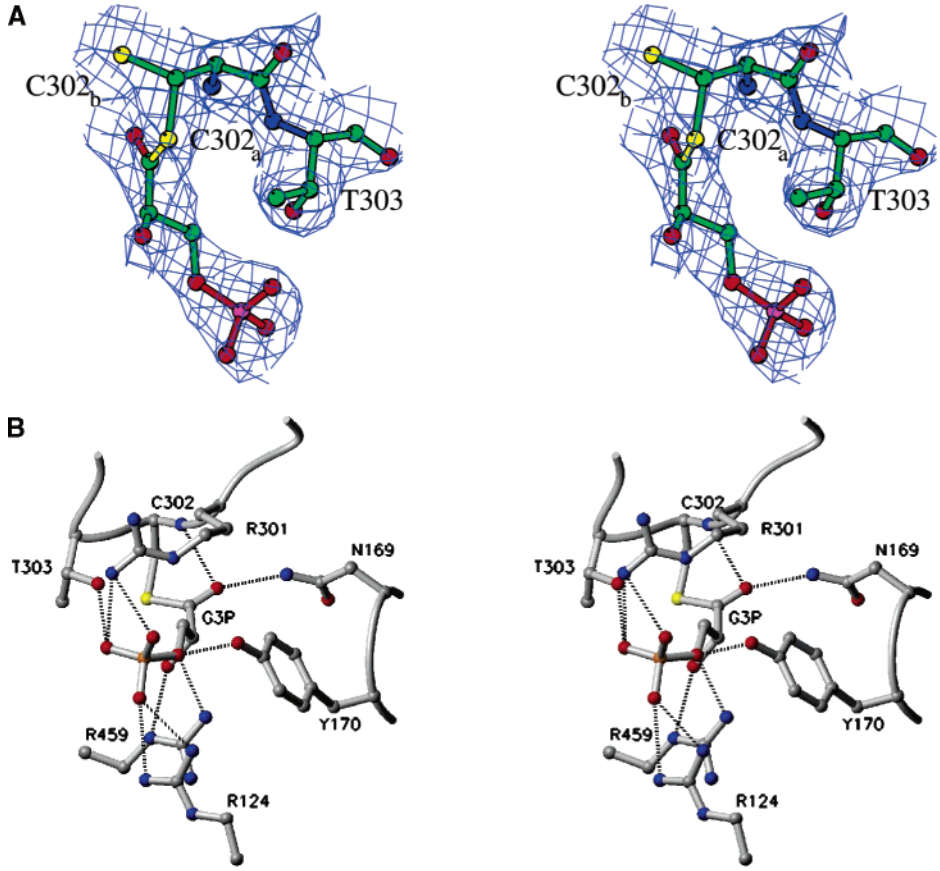

FIGURE 1: Steroview of the active site. (A) View of the D-G3P molecule in the E268A/NADP/G3P complex (monomer C) in the ($3F_o - 2F_c$) electron-density map (contour level, 1.0σ). The two conformations of the catalytic cysteine (in yellow) are represented: C302a (cysteine side chain bonded to the substrate) and C302b (free cysteine side-chain conformation). (B) View of the active site showing the interactions shared between D-G3P and the protein residues.

Table 2: Interactions between the Substrate, D-G3P, and the Active-Site Residues[a]

substrate atoms	thioacylenzyme (E268A−GapN)	C302S−GapN/cofactor/substrate noncovalent ternary complex
O1	N169−ND_2 (2.77 Å)	N169−ND_2 (3.46 Å)
	C302−NH (2.75 Å)	S302−NH (3.78 Å)
O2	R459−NE (2.65 Å)	R459−NE (3.74 Å)
O1P	Y170−OH (3.17 Å)	Y170−OH (3.33 Å)
	−	T303−OG1 (2.94 Å)
	R459−NH[b] (3.59 Å)	−
O2P	R301−NH[b] (2.56 Å)	−
O3P	T303−OG1 (2.39 Å)	T303−OG1 (3.36 Å)
	R301−NH[b] (3.10 Å)	R301−NH[b] (2.86 Å)
O4P	R124−NH[b] (2.86 Å)	−
	R124−NH[c] (3.16 Å)	*R124−NH[c] (3.95 Å)*
	−	R459−NH[b] (3.25 Å)

[a] Values in italics do not refer to an interaction but are indicated for comparative purposes. [b] This study. [c] From ref *11*.

is hydrogen-bonded to the R459−NE (2.65 Å) atom. The phosphate group at C3 is well-oriented to develop interactions with the guanidinium group of three arginine residues found in the neighborhood of the active site (R124, R301, and R459), together with the side chains of Y170 and T303 (Figure 1B). Altogether, the residues that share interactions with the substrate are the same as those depicted to be involved in its binding in the noncovalent C302S/$NADP^+$/G3P complex (*11*). Nonetheless, the interaction pattern and atom distances are different (Table 2). Moreover, the interactions observed here are consistent with the conclusions drawn by Marchal and Branlant (*29*) from kinetic results obtained on the R124L, R301L, and R459I GAPNs.

Evidence for Cofactor Reduction within the Crystals. As a first approach to characterize the redox state of the cofactor within the crystalline ternary complex, microspectrofluorimetry experiments were performed on single crystals of E268A−GAPN holoform before and after incubation with the substrate, D-G3P. However, single crystals of the holoenzyme in the absence of D-G3P exhibited unexplained fluorescence emission spectra whose shape and intensity in the 400−500 nm region prevented any subsequent measurement of spectral changes caused by NADPH production during the acylation process. This fluorescence emission is not due to a charge-transfer complex between the catalytic C302 and the NMN moiety of the $NADP^+$. Indeed, no absorption band is observed between 330 and 360 nm, and alkylation of the C302 by iodoacetamide (results not shown) does not abolish the fluorescence emission. The simultaneous quantification of the oxidized and reduced forms of the cofactor within the crystals was therefore carried out by HPLC analysis. For crystals soaked with G3P, a NADPH/$NADP^+$ ratio of 24 was found and clearly established that the acylation process took place within the crystals. Indeed, given the very strict substrate specificity of GAPN, the formation of NADPH cannot arise from other aldehydes that might have been present in the crystallization solution and reacted during the time course of the crystallization experiment. This point was further confirmed by control experi-

Table 3: Polar Interactions between the Cofactor and Neighboring Residues[a]

NADP	E268A/NADP/G3P ConfA	E268A/NADP/G3P ConfB	C302S/NADP/G3P
NA6	D229−OD2 (2.75 Å)	D229−OD2 (2.75 Å)	D229−OD2 (3.24 Å)
OA2*	K192−NZ (3.13 Å)	K192−NZ (3.13 Å)	K192−NZ (2.82 Å)
OAP2	T195−NH (2.75 Å)	T195−NH (2.75 Å)	T195−NH (2.68 Å)
	wat 630 (2.77 Å)	wat 630 (2.77 Å)	
OAP3	G226−NH (3.12 Å)	G226−NH (3.12 Å)	G226−NH (3.34 Å)
	T195−OG1 (2.54 Å)	T195−OG1 (2.54 Å)	T195−OG1 (3.13 Å)
OA3*	S166−O (3.32 Å)	S166−O (2.96 Å)	S166−O (3.09 Å)
			K192−NZ (3.54 Å)
OA1	S246−OG (2.66Å)	S246−OG (2.60 Å)	S246−OG (2.75 Å)
		S246−NH (2.60 Å)	S246−NH (3.02 Å)
OA2	wat 248 (2.74 Å)	wat 248 (3.18 Å)	
O3		S246−NH (3.38 Å)	S246−NH (3.47 Å)
			S246−OG (3.64 Å)
ON1	wat 248 (2.93 Å)	wat 248 (3.24 Å)	
ON2		F168−NH (3.16 Å)	
ON2*		E399−OE1 (2.61 Å)	E399−OE1 (3.65 Å)
ON3*		L267−CO (3.60 Å)	

[a] Because the reduced nicotinamide ring is not very well-defined in the electron-density map, putative interactions with the protein residues are not listed.

ments with unsoaked crystals for which no NADPH was detected.

Conformation of the Reduced Cofactor Molecule. The conformation of the oxidized $NADP^+$ molecule and its interactions with the enzyme has been described for the wild-type enzyme by Cobessi et al. (*15*). As found for other ALDHs (*14*, *16*, *30*, *31*), the cofactor straddles the Rossmann fold. The adenosine moiety is bond in a hydrophobic pocket located between helices α_7 and α_8, while the nicotinamide moiety is surrounded by the loop connecting β-strand J to α-helix 8, the loop located between the helix α_9 and the β-strand M, containing the catalytic C302, and the loop connecting the cofactor-binding domain to the catalytic one.

In the structure described here, the adenosine 2′-phosphate mononucleotide phosphate moiety of the NADPH molecule is well-defined in the $(3F_o - 2F_c)$ electron-density maps in the four monomers. It adopts a unique conformation with full occupancy and develops the same interactions with the protein residues (Table 3) as those already described for the wild-type holoenzyme (*15*) and in the noncovalent ternary complex (*11*). The electron density in the difference maps becomes poorer from the NMNH phosphate group to the nicotinamide ring, which highlights that the NMNH moiety is more disordered. Nevertheless, the electron density still clearly shows two positions for the NMNH phosphate group and allowed us to built two conformations (called ConfA and ConfB, Figure 2), which were refined with an occupancy factor of 0.5 each. Between these two conformations, the position of the phosphate of the NMNH moiety is shifted 1.5 Å and two rotations bring the ribose of the NMNH moiety at two radically different positions, in which the two O3* atoms and the two O2* atoms are separated by 11.3 and 9.1 Å, respectively (Figure 2). The switch between ConfA and ConfB is allowed by a 90° rotation around the NP−05* bond and a 110° rotation around the 05*−C5* bond. In ConfA, the ribose of the NMNH moiety and the nicotinamide point toward the protein surface, while they are more bulky in ConfB.

The main point here is that, whatever the conformation considered, the positioning of the NMNH moiety differs clearly from that of the NMN moiety depicted for the noncovalent C302S/$NADP^+$/G3P ternary complex[2] (Figure 3) (*11*) or for other ALDHs (*16*−*18*). When compared to the noncovalent ternary complex, ribose of the NMNH moiety rotated in ConfA nearly 70° around the NP−O5* bond and rotated in ConfB approximately 120° around the C4*−C5* bond.

DISCUSSION

Crystal structures of several members of the ALDH superfamily have revealed an apparent flexibility for the NMN(H) moiety of the cofactor. This flexibility has been hypothesised to constitute an essential feature of the catalytic mechanism and to be correlated with the two-step mechanism, because the conformation of the cofactor required for the acylation step is not appropriate to allow the conserved E268 to position and activate the water molecule for nucleophilic attack on the thioacylenzyme intermediate during the deacylation step.

This paper describes for the first time the structure of a covalent ternary complex corresponding to the thioacyl-enzyme intermediate for a member of the ALDH superfamily and provides strong structural evidence of the conformational changes of the cofactor molecule required for the deacylation step. To obtain this complex, we used a GAPN enzyme, in which the active-site E268 was substituted by an alanine. The crystals of the E268A−GAPN were grown in the presence of an excess of $NADP^+$ and soaked in the mother liquor containing the substrate prior to flash-freezing. HPLC analyses assessed that reduction of the cofactor had indeed occurred within the crystal. The ternary complex structure reveals that the substrate is bound in the four monomers and possesses the geometric features expected for a thioacyl-enzyme intermediate. It highlights that reduction of the coenzyme leads to an extensive motion of the NMNH moiety, undescribed thus far, which shifts the reduced pyridinium ring away from the active site.

Double Conformation of the Catalytic C302 and NADPH. As described in the Results, the catalytic C302 and the NMNH moiety of the cofactor both adopt two conformations in each monomer of the present structure. In regard to the catalytic C302, electron-density map analysis allowed us to assign one conformation to the cysteine side chain bonded to the substrate and the second one to the free cysteine side chain. Although this second conformation could have been explained as first glance by the presence of a population of enzyme molecules that has not undergone the catalytic process, this hypothesis seems rather unlikely for the following reasons. First, the acylation rate is fast (210 s^{-1} in the solution state and should still be efficient in the crystalline state), and analysis of the electron-density map did not allow us to observe the presence of $NADP^+$ in the hydride-transfer position, as expected if the acylation step had not occurred yet. Second, the NADPH/$NADP^+$ ratio of 24 strongly supports cofactor reduction within the crystals.

[2] Note that, in this former structure, the nicotinamide ring that was not well-defined in the electron-density map had been placed in syn instead of the anti position expected from the stereospecificity of hydride transfer. However, it does not change the conclusion drawn here because, whatever the position, syn or anti, the NMN moiety adopts a conformation incompatible with the deacylation step.

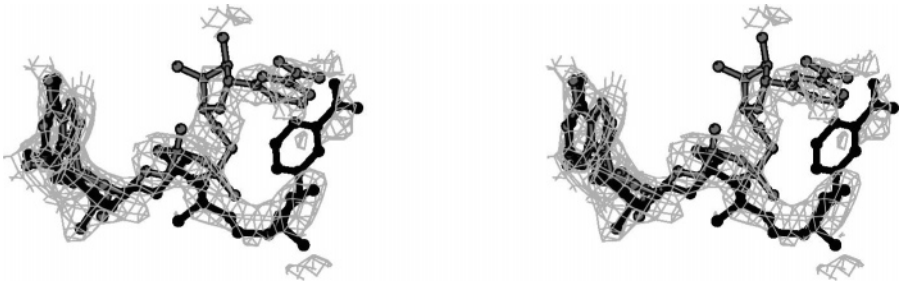

FIGURE 2: Stereoview of the two conformations of the cofactor molecule (monomer C) in a ($3F_o - 2F_c$) electron-density map (contour level, 1σ). In black, ConfB; and in light gray, ConfA.

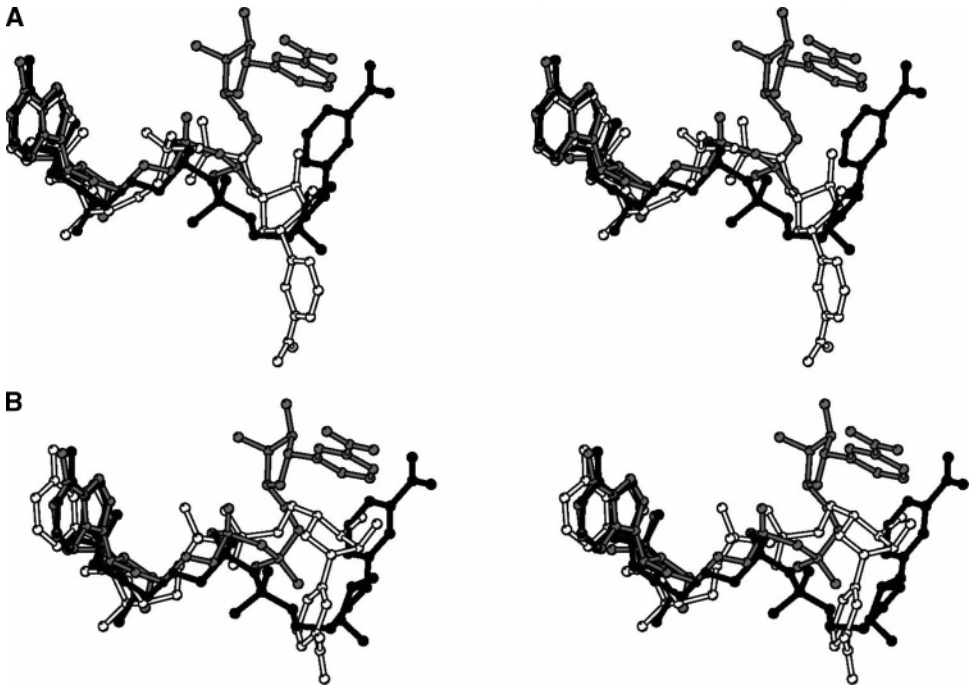

FIGURE 3: Stereoview of the two NADPH conformations (in black, ConfB; and in light gray, ConfA) superimposed (A) with $NADP^+$ in the noncovalent ternary complex (represented in white, from ref *11*) and (B) with NADH as observed in the human ALDH2/NADH binary complex (represented in white, from ref *18*).

Third, the observed conformation of C302 is not the one found in the holoenzyme structure but in the apostructure while the cofactor is bound with a full occupancy. Given that GAPN from *S. mutans* follows the same ordered sequential mechanism as human or other ALDHs (*4*, *5*), where NAD(P)H release constitutes the last step of the reaction after product release, these observations therefore suggest that this conformation of C302 is rather corresponding to an enzyme population for which the reaction has reached a further stage, including hydrolysis of the thioacylenzyme and subsequent product release, but where the reduced coenzyme is still bound.

Conformation of the NMN(H) Moiety and Comparison with Those Found in Other ALDH Structures. Crystal structures of human ALDH2 in the binary complex with either NAD^+ or NADH showed that the oxidized form of the coenzyme rather adopts an extended conformation compatible with the hydride transfer, whereas the reduced form exhibits a contracted conformation that was hypothesized to be suitable for enzyme hydrolysis (*18*). In the case of GAPN, the structure of a noncovalent ternary complex, C302S/$NADP^+$/G3P (*11*), already reported the conformation of $NADP^+$ at the ground-state level (Michaelis complex). In this structure, the substrate was well-oriented for an efficient acylation step, but as observed for human ALDH2, this conformation could not be suitable for the deacylation

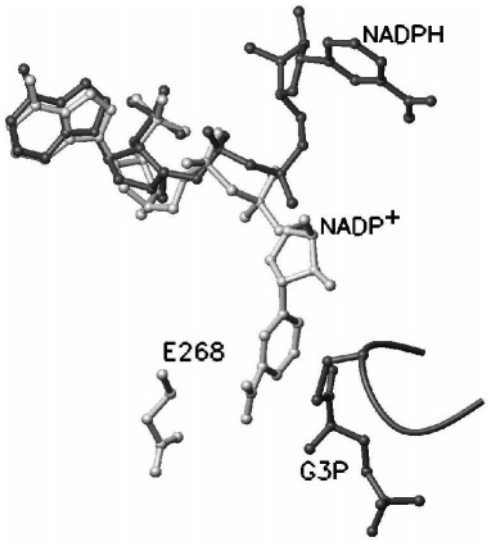

FIGURE 4: Superimposition of the noncovalent ternary complex (hydride transfer conformation, *11*) and the thioacylenzyme intermediate (ConfA, this study) showing the cofactor conformation during the acylation and deacylation steps.

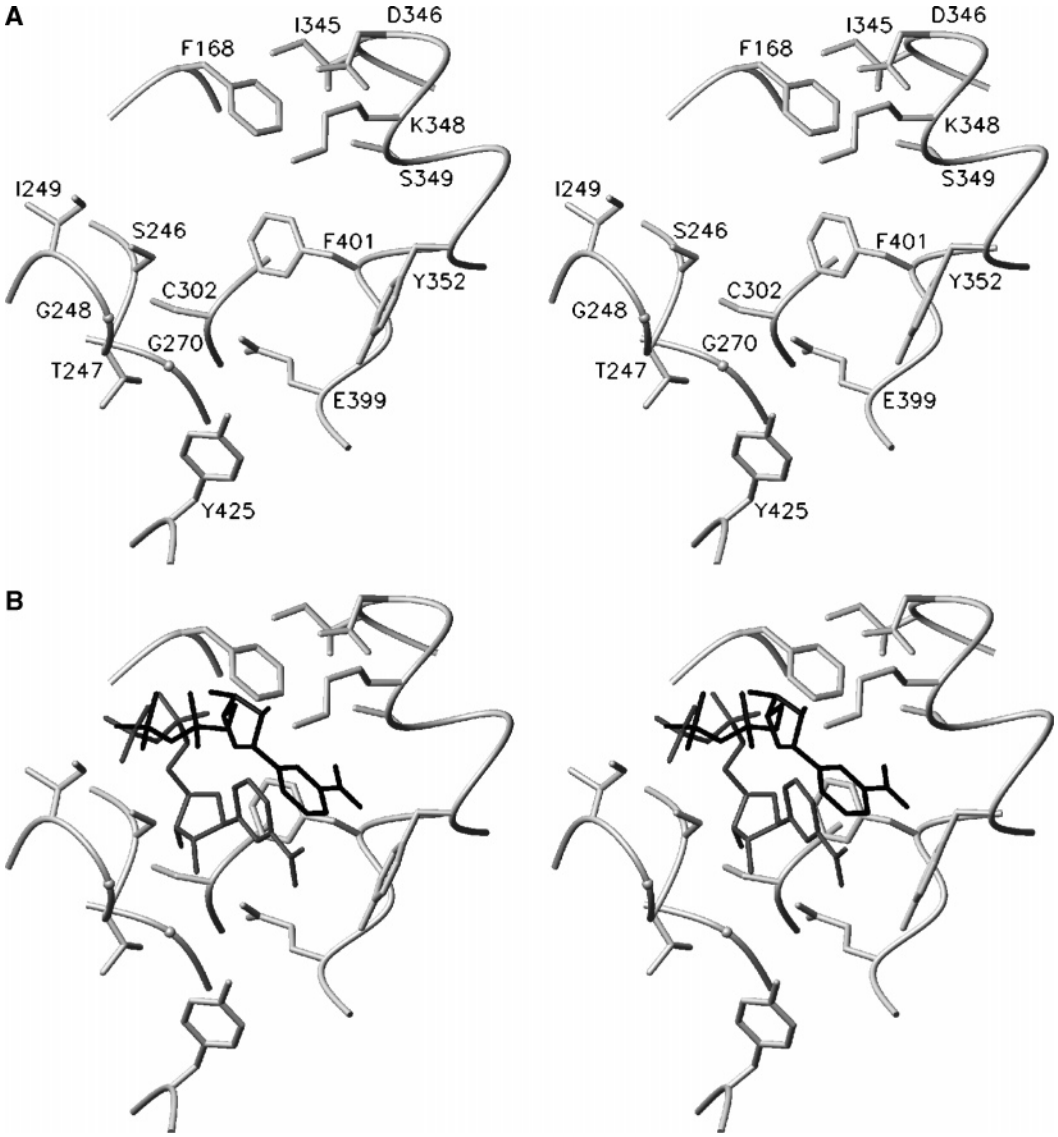

FIGURE 5: Stereoview of the cavity constituting the binding pocket of the NMNH moiety (A) in the absence of the cofactor and (B) with the two conformations of the reduced cofactor molecule.

step because the nicotinamidium ring blocks the way and prevents E268 to position and activate the water molecule for the deacylation step (Figure 4). Because NADPH release constitutes the last step of the reaction, it seemed reasonable to postulate that, in GAPN−ALDH, the NMNH moiety must also be displaced for a proper activation of the deacylating water molecule by residue E268 in the second step of the reaction (deacylation step).

In the present structure that can be described as a mixture of a thioacylenzyme intermediate and a binary enzyme/NADPH complex, the conformations found for the NMNH moiety of NADPH indeed differ from that observed for the NMN moiety of $NADP^+$ in the Michaelis complex C302S/NADP/G3P and are shifted away from the catalytic site. Moreover, their positioning strongly differ from the "hydrolysis" conformation described by Perez-Miller and Hurley (*18*) for human ALDH2 in complex with NADH (Figure 3B). Although this difference might only further reflect the high mobility of the NMNH moiety that can adopt multiple alternative conformations, a thorough comparison between the two structures reveals that, in the human ALDH2 binary NADH complex, the oxygen atom of the amidic group from the reduced pyridinium (NO7 atom) is postulated to be hydrogen-bonded to the side chain of N169. In contrast, in the GAPN thioacylenzyme intermediate, the oxygen atom at C1 of the substrate occupies this position and interacts with the N169−ND2 atom, which is known to constitute, together with the catalytic C302 amide nitrogen, the oxyanion hole required not only for the hydride transfer but also for the stabilization of the different intermediates during the catalytic cycle. On the basis of the modeling experiment, Perez-Miller and Hurley (*18*) suggested that the hydrolysis conformation of NADH in ALDH2 might be compatible with an acylated enzyme species. In our case, reduction of the coenzyme molecule has occurred within the crystals in the presence of the natural substrate. Therefore, this structure likely constitutes a reasonable picture of the thioacylenzyme intermediate for the physiological reaction.

Isomerization of the NMN(H) Moiety of the Cofactor Molecule. In the noncovalent ternary complex (*11*) representative of the hydride transfer conformation, the nicotinamide ring was flanked by the side chain of the catalytic

C302 on one side and by the side chain of residue T244 on the other side. Once the thioacylenzyme has been formed and the cofactor has been concomitantly reduced (this study), the NMNH moiety is found in a cavity, delineated by residues F168, S246−I249, G270, I345, D346, K348, S349, Y352, E399−F401, and Y425 (Figure 5). Superimposition of the structures of these two complexes highlights the fact that the NMNH movement does not require any noticeable conformational change of the protein structure. This is probably explained by the peculiar mode of binding of the cofactor in this family (*11* and references therein) and by the fact that the cavity is wide enough to accommodate the NMNH moiety. Inspection of the 3D structures currently available reveals that this cavity is also present in other nonphosphorylating CoA-independent ALDHs and involves conserved residues. We therefore propose that it constitutes the pocket occupied by the NMNH moiety during the deacylation step for the other members of the nonphosphorylating CoA-independent ALDH family. Because this cavity opens to the exterior, it might constitute the exit door for NAD(P)H as well.

As already mentioned, the isomerization of the cofactor should occur after the oxidoreduction step to allow the catalytic E268 to play its role in the deacylation step. This is supported by the relative positioning of the NMN moiety of $NADP^+$ toward E268 as deduced from the inspection of the 3D structures of numerous ALDH−$NAD(P)^+$ (*13*−*17*) complexes and of the ternary complex C302S GAPN−$NADP^+$−G3P (*11*). The latter complex is likely representative of the structure of the wild-type ternary Michaelis complex. Indeed, using W397 as a conformational kinetic probe, binding of G3P to the C302S GAPN−$NADP^+$ complex was shown to induce a conformational reorganization of the active site similar to that observed on C302A GAPN (*32* and unpublished results) and on the wild type. Nonetheless, the question concerning the molecular factors and the driving force, which promote isomerization of the cofactor, remains to be addressed. In the binary complex GAPN−$NADP^+$, it is probable that the presence of the thiolate form of C302 near the positive charge of the pyridinium ring of $NADP^+$ is one of the factors that favors a NMN moiety conformation suitable for hydride transfer. However, in the transient thiohemiacetal enzyme intermediate in which C302 is engaged in a covalent linkage, additional interactions should stabilize the $NADP^+$ "hydride" conformation. One of them could be the negative charge of the oxyanion of the thiohemicetal intermediate, which is never protonated within the active site. Moreover, as soon as the hydride transfer occurs, the loss of the positive charge of the pyridinium ring and the nonplanar conformation of the dihydropyridine ring likely participate in triggering the NMNH conformational isomerization process. However, a low energetic barrier is likely existing between the conformations adopted by NADP(H) within GAPN during the catalytic cycle. Indeed, we recently solved the structure of a GAPN mutant protein in complex with $NADP^+$, in which the catalytic C302 has been substituted by an arginine (D'Ambrosio et al., unpublished data), a residue naturally encountered at this position in some Ω crystallins (*33*, *34*). In this structure, the R302 residue was found to mimic quite well the shape of the substrate covalently bond to the catalytic C302, and surprisingly enough, we observed that despite the oxidized state of the cofactor, its NMN moiety was located in the same position as that depicted here for the NMNH moiety in the thioacylenzyme structure.

Evolutionary Viewpoint. The data presented above show how the NMN(H) moiety of the cofactor displays different conformations throughout the catalytic cycle of GAPN. This likely constitutes a specific feature of all nonphosphorylating CoA-independent ALDHs. In the "hydride-transfer" conformation, the positioning of the NMN moiety prevents the E268 from playing its role in the deacylation process. Therefore, either the NMNH moiety flips or the reduced cofactor dissociates before the hydrolysis process. Clearly, our structural study supports the "flipping" mechanism that is also in accordance with the ordered sequential nature of the kinetic mechanism in which NAD(P)H dissociates last. The picture is clearly different for other ALDH families. Indeed, for the phosphorylating glyceraldehyde-3-phosphate dehydrogenase (GAPDH), which is a representative member of the phosphorylating ALDH family, characterization of its mechanistic and structural properties has highlighted major differences in terms of cofactor binding mode and kinetic mechanism. First, the NAD(H) binding mode to the canonical Rossmann fold does not allow the NMN(H) moiety to adopt different conformations during the two-step mechanism. Second, kinetic data support a ping-pong mechanism in which a cofactor exchange step (NADH release/NAD^+ binding) precedes the nucleophilic attack by inorganic phosphate (*35*), although there is no steric hindrance that can prevent the phosphorolysis of the thiacylenzyme/NADH complex. In fact, the cofactor exchange step would be a prerequisite for accelerating the rate of phosphorolysis by increasing the reactivity of the thioacylenzyme intermediate toward inorganic phosphate. Finally, kinetic data obtained on two members of the nonphosphorylating CoA-dependent ALDH family, i.e., the acetaldehyde dehydrogenase and the succinate semialdehyde dehydrogenase, support a ping-pong mechanism in which NADH release precedes CoA binding (*2*, *3*). Whether the reduced cofactor blocks the way for the nucleophilic attack by the CoA molecule or NADH and CoA binding sites overlap, at least partially, remains to be determined. From the three examples cited above, it clearly appears that evolution has led to different solutions to achieve a similar two-step mechanism in ALDHs.

REFERENCES

1. Segal, H. L., and Boyer, P. D. (1953) The role of sulfhydryl groups in the activity of D-glyceraldehyde-3-phosphate dehydrogenase, *J. Biol. Chem.* 204, 265−281.
2. Shone, C. C., and Fromm, H. J. (1981) Steady-state and pre-steady-state kinetics of coenzyme A linked aldehyde dehydrogenase from *Escherichia coli*, *Biochemistry 20*, 7494−7501.
3. Söhling, B., and Gottschalk, G. (1993) Purification and characterization of a coenzyme-A-dependent succinate−semialdehyde dehydrogenase from *Clostridium kluyveri*, *Eur. J. Biochem. 212*, 121−127.
4. Marchal, S., Rahuel-Clermont, S., and Branlant, G. (2000) Role of glutamate-268 in the catalytic mechanism of nonphosphorylating glyceraldehyde-3-phosphate dehydrogenase from *Streptococcus mutans*, *Biochemistry 39*, 3327−3335.
5. Sheikh, S., Ni, L., Hurley, T. D., and Weiner, H. (1997) The potential roles of the conserved amino acids in human liver mitochondrial aldehyde dehydrogenase, *J. Biol. Chem.* 272, 18817−18822.
6. Farres, J., Wang, T. T., Cunningham, S. J., and Weiner H. (1995) Investigation of the active site cysteine residue of rat liver

mitochondrial aldehyde dehydrogenase by site-directed mutagenesis, *Biochemistry 34*, 2592−2598.
7. Vedadi, M., Szittner, R., Smillie, L., and Meighen E. (1995) Involvement of cysteine 289 in the catalytic activity of an $NADP^+$-specific fatty aldehyde dehydrogenase from *Vibrio harveyi*, *Biochemistry 34*, 16725−16732.
8. Wang, X., and Weiner, H. (1995) Involvement of glutamate 268 in the active site of human liver mitochondrial (class 2) aldehyde dehydrogenase as probed by site-directed mutagenesis, *Biochemistry 34*, 237−243.
9. Vedadi, M., and Meighen E. (1997) Critical glutamic acid residues affecting the mechanism and nucleotide specificity of *Vibrio harveyi* aldehyde dehydrogenase, *Eur. J. Biochem. 246*, 698−704.
10. Marchal, S., and Branlant, G. (1999) Evidence for the chemical activation of essential Cys-302 upon cofactor binding to nonphosphorylating glyceraldehyde 3-phosphate dehydrogenase from *Streptococcus mutans*, *Biochemistry 38*, 12950−12958.
11. Cobessi, D., Tête-Favier, F., Marchal, S., Branlant, G., and Aubry, A. (2000) Structural and biochemical investigations of the catalytic mechanism of an NADP-dependent aldehyde dehydrogenase from *Streptococcus mutans*, *J. Mol. Biol. 300*, 141−152.
12. Marchal, S., and Branlant, G. (2001) Engineered nonphosphorylating glyceraldehyde 3-phosphate dehydrogenase at position 268 binds hydroxylamine and hydrazine as acyl acceptors, *Eur. J. Biochem. 268*, 5764−5770.
13. Liu, Z. J., Sun, Y. J., Rose, J, Chung, Y. J., Hsiao, C. D., Chang, W. R., Kuo, I., Perozich, J., Lindahl, R., Hempel, J., and Wang, B. C. (1997) The first structure of an aldehyde dehydrogenase reveals novel interactions between NAD and the Rossmann fold, *Nat. Struct. Biol. 4*, 317−326.
14. Johansson, K. El-Ahmad, M. Ramaswamy, S., Hjelmqvist, L., Jörnvall, H., and Eklund, H. (1998) Structure of betaine aldehyde dehydrogenase at 2.1 Å resolution, *Protein Sci. 7*, 2106−2117.
15. Cobessi, D., Tête-Favier, F., Marchal, S., Azza, S., Branlant, G., and Aubry, A. (1999) Apo and holo crystal structures of an NADP-dependent aldehyde dehydrogenase from *Streptococcus mutans*, *J. Mol. Biol. 290*, 161−173.
16. Steinmetz, C. G., Xie, P., Weiner, H., and Hurley, D. T. (1997) Structure of mitochondrial aldehyde dehydrogenase: The genetic component of ethanol aversion, *Structure 5*, 701−711.
17. Moore, S. A., Baker, H. M., Blythe, T. J., Kitson, K. E., Kitson, T. M., and Baker, E. N. (1998) Sheep liver cytosolic aldehyde dehydrogenase: The structure reveals the basis for the retinal specificity of class 1 aldehyde dehydrogenases, *Structure 6*, 1541−1551.
18. Perez-Miller, S. J., and Hurley, T. D. (2003) Coenzyme isomerization is integral to catalysis in aldehyde dehydrogenase, *Biochemistry 42*, 7100−7109.
19. Lorentzen, E., Hensel, R., Knura, T., Ahmed, H., and Pohl, E. (2004) Structural basis of allosteric regulation and substrate specificity of the non-phosphorylating glyceraldehyde 3-phosphate dehydrogenase from *Thermoproteus tenax*, *J. Mol. Biol. 341*, 815−828.
20. Roth, M., Carpentier, P., Kaikati, O., Joly, J., Charrault, P., Pirocchi, M., Kahn, R., Fanchon, E., Jacquamet, L., Borel, F., Bertoni, A., Israel-Gouy, P., and Ferrer, J. L. (2002) FIP: A highly automated beamline for multiwavelength anomalous diffraction experiments, *Acta Crystallogr., Sect. D: Biol. Crystallogr. 58*, 805−814.
21. Otwinowski, Z., and Minor, W. (1997) Processing of X-ray diffraction data collected in oscillation mode, *Methods Enzymol. 276*, 307−326.
22. Brünger, A. T., Adams, P. D., Clore, G. M., DeLano, W. L., Gros, P., Grosse-Kunsteleve, R. W., Jiang, J. S., Kuszewski, J., Nilges, M., Pannu, N. S., Read, R. J., Rice, L. M., Simonson, T., and Warren, G. L. (1998) Crystallography and NMR system: A new software suite for macromolecular structure determination, *Acta Crystallogr., Sect. D: Biol. Crystallogr. 54*, 905−921.
23. Roussel, P. A., and Cambillau, C. (1991) TURBO−FRODO, Silicon Graphics Applications Directory, Silicon Graphics, Mountain View, CA.
24. Laskowsky, R. A. MacArthur, M. W. Moss, D. S., and Thornton, J. M. (1993) PROCHECK: A program to check the stereochemical quality of protein structures, *J. Appl. Crystallogr. 26*, 283−291.
25. Esnouf, R. M. (1999) Further additions to MolScript version 1.4, including reading and contouring of electron-density maps, *Acta Crystallogr., Sect. D: Biol. Crystallogr. 55*, 938−940.
26. Koradi, R., Billeter, M., and Wuthrich, K. (1996) MOLMOL: A program for display and analysis of macromolecular structures, *J. Mol. Graphics 14*, 51−55.
27. Brzozowski, A. M., and Walton, J. (2001) Clear strategy screens for macromolecule crystallisation, *J. Appl. Crystallogr. 34*, 97−101.
28. Rossmann, M. G., Moras, D., and Olsen, K. W. (1974) Chemical and biological evolution of nucleotide-binding protein, *Nature 250*, 194−199.
29. Marchal, S., and Branlant, G. (2002) Characterization of the amino acids involved in substrate specificity of nonphosphorylating glyceraldehyde-3-phosphate dehydrogenase from *Streptococcus mutans*, *J. Biol. Chem. 277*, 39235−39242.
30. Lamb, A. L., and Newcomer, M. E. (1999) The structure of retinal dehydrogenase type II at 2.7 Å resolution: Implications for retinal specificity, *Biochemistry 38*, 6003−6011.
31. Ahvazi, B., Coulombe, R., Delarge, M., Vedadi, M., Zhang, L., Meighen, E., and Vrielink, A. (2000) Crystal structure of the $NADP^+$-dependent aldehyde dehydrogenase from *Vibrio harveyi*: Structural implications for cofactor specificity and affinity, *Biochem. J. 349*, 853−861.
32. Marchal, S., Cobessi, D., Rahuel-Clermont, S., Tête-Favier, F., Aubry, A., and Branlant, G. (2001) Chemical mechanism and substrate bindin sites of NADP-dependent aldehyde dehydrogenase from *Streptococcus mutans*, *Chem.-Biol. Interact. 130−132*, 15−28.
33. Montgomery, M. K., and McFall-Ngai, M. J. (1992) The muscle-derived lens of a squid bioluminescent organ is biochemically convergent with the ocular lens. Evidence for recruitment of aldehyde dehydrogenase as a predominant structural protein, *J. Biol. Chem. 267*, 20999−21003.
34. Zinovieva, R. D., Tomarev, S. I., and Piatigorsky, J. (1993) Aldehyde dehydrogenase-derived ω-crystallins of squid and octopus. Specialization for lens expression, *J. Biol. Chem. 268*, 11449−11455.
35. Harrigan, P. J., and Trentham D. R. (1974) Kinetic studies on oxidized nicotinamide−adenine dinucleotide-facilitated reactions of D-glyceraldehyde 3-phosphate dehydrogenase, *Biochem. J. 143*, 353−363.

BI0515117